Article

Cell Reports

# Increased 4E-BP1 Expression Protects against Diet-Induced Obesity and Insulin Resistance in Male Mice

## Graphical Abstract

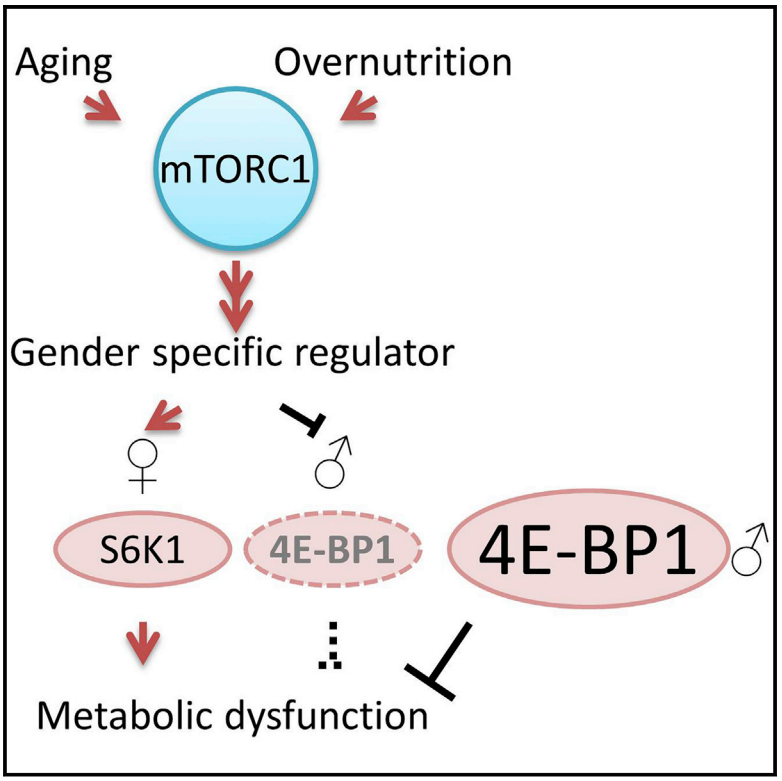


## Authors

Shih-Yin Tsai, Ariana A. Rodriguez, Somasish G. Dastidar, ..., Travis D. Ashe, Albert R. La Spada, Brian K. Kennedy

## Correspondence

alaspada@ucsd.edu (A.R.L.S.), bkennedy@buckinstitute.org (B.K.K.)

## In Brief

Tsai et al. identify gender-specific differences in the mTOR pathway when animals are challenged with a high-fat diet or during aging-related obesity. The level of one mTOR substrate, 4E-BP1, declined under these conditions in males, and enhancing its levels using a transgenic approach suppresses male metabolic defects.

## Highlights

- There are gender differences in the expression of 4E-BP1 upon overnutrition
- 4E-BP1 is a gender-specific suppressor of metabolic dysfunction
- Transgenic 4E-BP1 male mice are protected from age-induced metabolic dysfunction

Tsai et al., 2016, Cell Reports *16*, 1903–1914
August 16, 2016 
http://dx.doi.org/10.1016/j.celrep.2016.07.029

CellPress

Cell Reports
Article



# Increased 4E-BP1 Expression Protects against Diet-Induced Obesity and Insulin Resistance in Male Mice

Shih-Yin Tsai,[1] Ariana A. Rodriguez,[1] Somasish G. Dastidar,[2] Elizabeth Del Greco,[1] Kaili Lia Carr,[1] Joanna M. Sitzmann,[1] Emmeline C. Academia,[1] Christian Michael Viray,[1] Lizbeth Leon Martinez,[1] Brian Stephen Kaplowitz,[1] Travis D. Ashe,[2] Albert R. La Spada,[2,3,*] and Brian K. Kennedy[1,*]

[1]Buck Institute for Research on Aging, Novato, CA 94945, USA
[2]Division of Biological Sciences, Departments of Pediatrics, Cellular and Molecular Medicine, and Neurosciences, Institute for Genomic Medicine, and Sanford Consortium for Regenerative Medicine, University of California, San Diego, La Jolla, CA 92903, USA
[3]Rady Children's Hospital, San Diego, CA 92123, USA
*Correspondence: alaspada@ucsd.edu (A.R.L.S.), bkennedy@buckinstitute.org (B.K.K.)
http://dx.doi.org/10.1016/j.celrep.2016.07.029

## SUMMARY

**Obesity is a major risk factor driving the global type II diabetes pandemic. However, the molecular factors linking obesity to disease remain to be elucidated. Gender differences are apparent in humans and are also observed in murine models. Here, we link these differences to expression of eukaryotic translation initiation factor 4E binding protein 1 (4E-BP1), which, upon HFD feeding, becomes significantly reduced in the skeletal muscle and adipose tissue of male but not female mice. Strikingly, restoring 4E-BP1 expression in male mice protects them against HFD-induced obesity and insulin resistance. Male 4E-BP1 transgenic mice also exhibit reduced white adipose tissue accumulation accompanied by decreased circulating levels of leptin and triglycerides. Importantly, transgenic 4E-BP1 male mice are also protected from aging-induced obesity and metabolic decline on a normal diet. These results demonstrate that 4E-BP1 is a gender-specific suppressor of obesity that regulates insulin sensitivity and energy metabolism.**

## INTRODUCTION

White adipose tissue is the major tissue that stores excess energy and regulates thermogenesis (Tseng et al., 2010; Wu et al., 2013). In addition, this tissue secretes several adipokines in the regulation of whole-body metabolic homeostasis and in response to chronic inflammation, the likely cause of insulin resistance (Samuel and Shulman, 2012; Tseng et al., 2010; Zeyda and Stulnig, 2007). Obesity induced by a high-fat diet (HFD) is associated with increased secretion of adipokines, such as tumor necrosis factor $\alpha$ and interleukin-6, and contributes to systemic inflammation and insulin resistance. The connections between obesity, adipokine secretion, and metabolic dysfunction remain to be understood.

Of individuals diagnosed with type II diabetes (T2D), nearly 80% are also obese. However, not all obese individuals will develop T2D (Carnethon et al., 2012; Cowie et al., 2010). Family history, age, and race all contribute to individual susceptibility to T2D, suggesting that genetic factors are involved in its onset. Genetic association studies have pinpointed many risk factors (Elbein et al., 2012; Lyssenko and Laakso, 2013; Morris et al., 2012; Williams et al., 2014), but it remains poorly understood why obesity drives metabolic dysfunction in some but not all cases.

In rodent models exposed to a HFD, gender dimorphism with respect to insulin resistance and glucose intolerance has also been reported (Grove et al., 2010; Macotela et al., 2009). A HFD induces a similar level of obesity in male and female mice, but the levels of anti-inflammatory signals are reported to be higher in female mice (Nickelson et al., 2012; Pettersson et al., 2012; Stubbins et al., 2012). This increase in anti-inflammatory signaling is correlated with maintenance of insulin sensitivity. The molecular basis for gender dimorphism is not yet fully understood.

The mammalian target of rapamycin (mTOR) kinase, a principal sensor that integrates nutrient levels to cell growth and proliferation, is a target downstream of insulin signaling (Dazert and Hall, 2011; Laplante and Sabatini, 2012). mTOR forms two functional complexes, mTOR complex 1 (mTORC1) and mTOR complex 2 (mTORC2). Activation of mTORC1 leads to the phosphorylation of the ribosomal S6 kinases (S6Ks) and 4E-BP (among other targets), which together induce ribosome biogenesis and mRNA translation (Sonenberg and Hinnebusch, 2009). mTORC1-dependent phosphorylation of 4E-BP results in dissociation of 4E-BP from eIF4E, specifically promoting cap-dependent translation initiation. Upregulation of mTORC1 signaling is often observed in tissues of obese individuals and mice and is associated with progressive insulin resistance (Cornu et al., 2013; Laplante and Sabatini, 2012). Reduced mTORC1 activity has been reported to prevent development of T2D and protect against diabetic nephropathy in both type I and type II diabetic mouse models (Gödel et al., 2011; Inoki et al., 2011; Polak et al., 2008; Um et al., 2004; Yang et al., 2007). However, the downstream target by which reduced

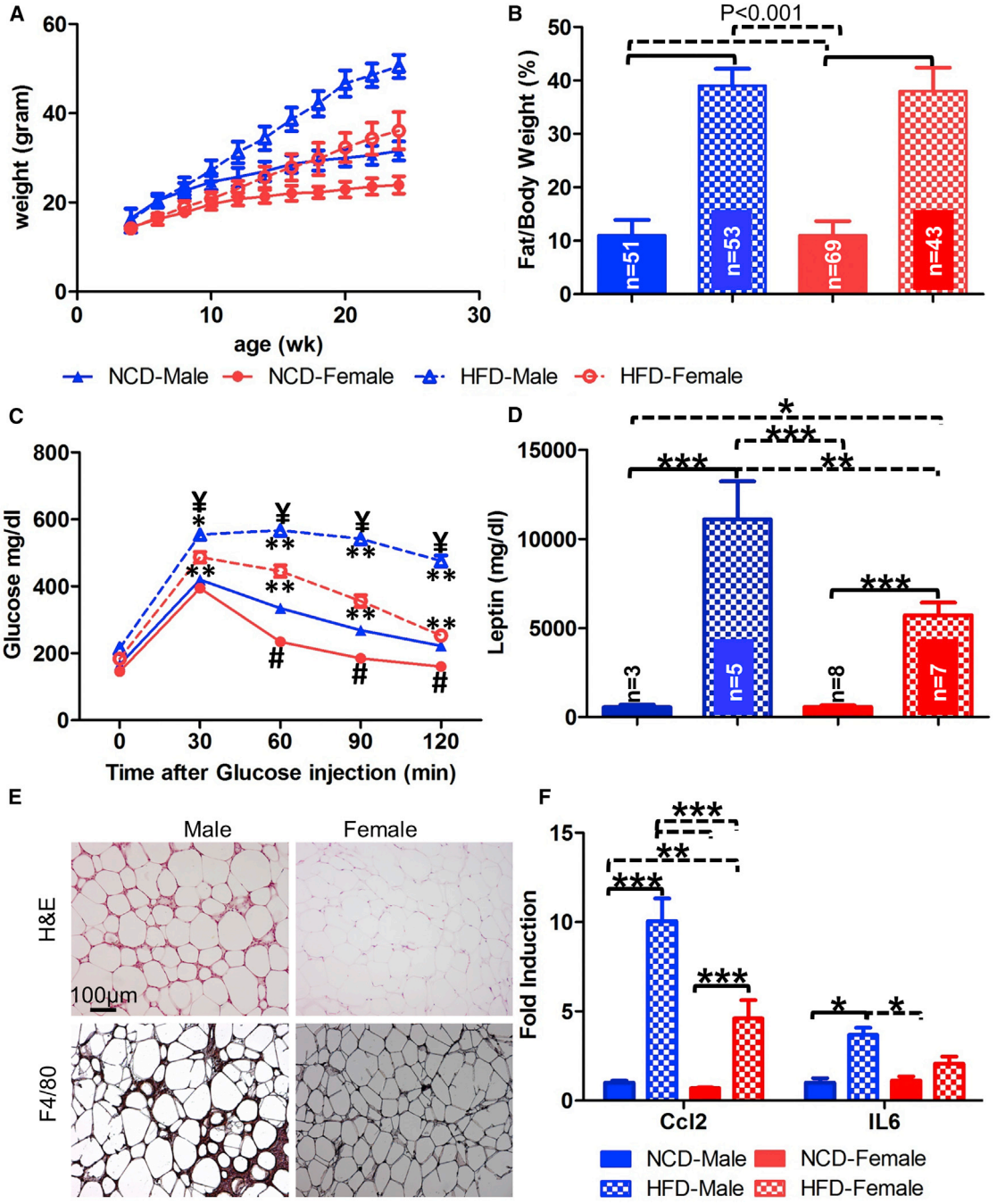


**Figure 1. Gender Dimorphism in Diet-Induced Insulin Resistance and Glucose Intolerance in the C57BL/6J Mouse Strain**

(A) Body weight measurement in wild-type C57BL/6J male and female mice on a normal chow diet and HFD (n = 20–53). $p < 0.001$ (NCD versus HFD: males started at 10 weeks and females started at 12 weeks). $p < 0.001$ (males versus females: NCD started at week 4). $p < 0.001$ (males versus females: HFD started at week 6).

(B) Fat mass measurement normalized with body weight in 6-month-old wild-type C57BL/6J male and female mice on a normal chow diet and HFD.

(C) Glucose tolerance assay in 6 hr-fasting wild-type C57BL/6J male and female mice on a normal chow diet and HFD (n = 36–44). *$p < 0.05$, **$p < 0.001$ (NCD versus HFD: same gender). #$p < 0.001$ (males versus females: NCD). ¥$p < 0.001$ (males versus females: HFD).

(D) Plasma leptin measurement in 6-month-old wild-type C57BL/6J male and female mice on a normal chow diet and HFD. The p values of the cross-comparison from the other groups were labeled as follows: *$p < 0.05$, **$p < 0.01$, ***$p < 0.001$.

(E) H&E (top) and F4/80 immunohistochemistry (IHC; bottom) staining of the visceral fat from 6-month-old HFD-fed wild-type male and female mice (n = 4∼7 for each group).

*(legend continued on next page)*

mTORC1 activity regulates whole-body metabolic homeostasis has not been determined.

Previously, 4E-BPs were shown to regulate adipogenesis and insulin sensitivity, making them strong candidates to link mTORC1 signaling and metabolism (Le Bacquer et al., 2007; Tsukiyama-Kohara et al., 2001). Whole-body deletion of 4E-BP1 and 4E-BP2 yields hypersensitivity to diet-induced obesity and insulin resistance. Here we report that gender differences in the expression of 4E-BP1 affect an individual's response to a normal and high-fat diet. The expression of 4E-BP1 is reduced specifically in male but not female skeletal muscle and adipose tissues on a HFD. This loss of expression has relevance because transgenic 4E-BP1 expression protects male mice specifically from diet-induced obesity and insulin resistance. Suppression of white adipose tissue accumulation is associated with reduced circulating free fatty acids as well as the secreted hormone leptin in male 4E-BP1 transgenic mice on a HFD. Similar results were obtained in aging mice, where 4E-BP1 transgenic expression protects aging male 4E-BP1 transgenic mice from aging-induced obesity and metabolic decline. These findings reveal that a previously unappreciated gender-specific regulation of 4E-BP1 underlies differential responses to overnutrition and that maintenance of 4E-BP1 function in male mice is important to offset the detrimental metabolic consequences of obesity.

## RESULTS

### Gender Dimorphism in a Diet-Induced Insulin Resistance Mouse Model

We sought to compare and contrast the impact of a HFD on obesity and metabolic dysfunction in male and female C57BL/6J mice. Mice from both genders were placed on either a normal calorie diet (NCD) (18% calories from fat) or a HFD (60% calories from fat) for 16 weeks beginning at 8 weeks of age. During this period, HFD-fed male mice gained 60% more weight than the NCD-fed cohort, whereas HFD-fed female mice gained 50% more weight than their NCD-fed cohort (Figure 1A). In general, males accumulated more adipose mass than females on either diet (Figure S1A), but both males and females had a similar level of obesity (approximately 38% adiposity) after 16 weeks on a HFD, as compared to NCD-fed mice (11% adiposity; Figure 1B).

Despite similar levels of obesity, male mice on a HFD had significantly higher fasting plasma glucose levels (Figure S1B) and developed more severe glucose intolerance and insulin resistance compared with female mice (Figure 1C; Figure S1C). HFD-fed male mice also had markedly increased serum leptin and triglyceride levels relative to females (Figure 1D; Figure S1D). In addition, there is a significant increase in macrophage accumulation in HFD-fed male mouse white adipose tissue (Figure 1E), which is correlated with induced pro-inflammatory gene expression (Figure 1F). Taken together, these data suggest that the intrinsic quality of adipose tissue is different in males and females on a HFD. Adipose tissues of HFD-fed male mice have enhanced secretion of factors that contribute to insulin resistance and glucose intolerance compared with adipose tissue in HFD-fed females.

Abnormal induction of mTORC1 signaling has been observed in response to insulin resistance and to be associated with diabetes progression (Cornu et al., 2013; Laplante and Sabatini, 2012). Thus, we examined whether the expression pattern of mTORC1 signaling downstream targets correlate with the gender dimorphism in diet-induced insulin resistance in C57BL/6J mice. Previously, upregulation of S6K1 signaling has been observed in diabetic tissues, and removal of S6K1 in mice has been reported to yield resistance to diet-induced obesity and insulin resistance (Um et al., 2004). Consistent with this phenotypic observation, we found that a target of S6K1, S6, is constitutively phosphorylated in both male and female mice on a HFD (Figures S1E and S1F). Although S6K1 signaling is active in both genders on a HFD, the mRNA expression and protein level of 4E-BP1 was significantly reduced in the skeletal muscle and adipose tissues of HFD-fed male mice. 4E-BP1 was less affected in females, with no significant difference in skeletal muscle. The basal level of 4E-BP1 expression is comparable in male and female mice on a normal diet, so the reduction of 4E-BP1 in male tissues is due to HFD feeding (Figure 2; Figures S2A–S2E). Although 4E-BP1 protein levels are comparable in female visceral fat between diets (Figure 2C; Figure S2B), 4E-BP1 protein is highly phosphorylated in visceral fat of HFD-fed female mice (Figures S2D and S2E). The levels of *4E-BP1* mRNA also become reduced in adipose tissues of HFD-fed female mice (Figure 2A). Phosphorylation of 4E-BP1 at mTORC1-regulated Thr37/46 site is slightly higher in tissues of HFD-fed mice (Figures S2D and S2E).

Next we examined possible mechanisms underlying sexual dimorphic regulation of 4E-BP1 expression. The expression of 4E-BP1 has been shown to be repressed by increased inflammatory signaling in vitro (Rolli-Derkinderen et al., 2003; Walsh et al., 2008; Weichhart et al., 2008). Moreover, sexual dimorphism in the inflammatory response has been reported in human obese subjects (Bloor and Symonds, 2014; Brown et al., 2010), in addition to our HFD-fed mice (Figures 1E and 1F). We hypothesized that the increased inflammation upon HFD feeding might be responsible for the decrease in 4E-BP1 expression. To test this, we treated primary mouse embryonic fibroblasts (MEFs) with an inflammatory agent, lipopolysaccharide (LPS), to acutely induce inflammation. Associated with the induction of phosphorylation of JNK, c-Jun N-terminal kinase (pJNK) signaling, 4E-BP1 is downregulated in LPS-treated MEFs (Figures S2F and S2G), suggesting that inflammation could be one of the factors regulating 4E-BP1 expression in diabetic tissue. This is consistent with a previous report that upregulation of the pJNK pro-inflammatory signaling pathway can repress 4E-BP1 expression in a pancreatic β cell line (Tominaga et al., 2010).

(F) Real-time PCR analysis of proinflammatory gene expression in visceral fat from 6-month-old normal diet-fed or HFD-fed male or female mice (n = 4). Fold induction was normalized to female normal diet-fed samples. The p values of the cross-comparison from the other groups were labeled as follows: $^{*}p < 0.05$, $^{**}p < 0.01$, $^{***}p < 0.001$.

All graphs are plotted as mean ± SEM of the number of mice used in each analysis. The numbers of samples analyzed are indicated. p Values were calculated by two-way ANOVA in (B), (D), and (F) and two-way ANOVA for repeated measures in (A) and (C), with Bonferroni post-tests to compare replicate means by row.

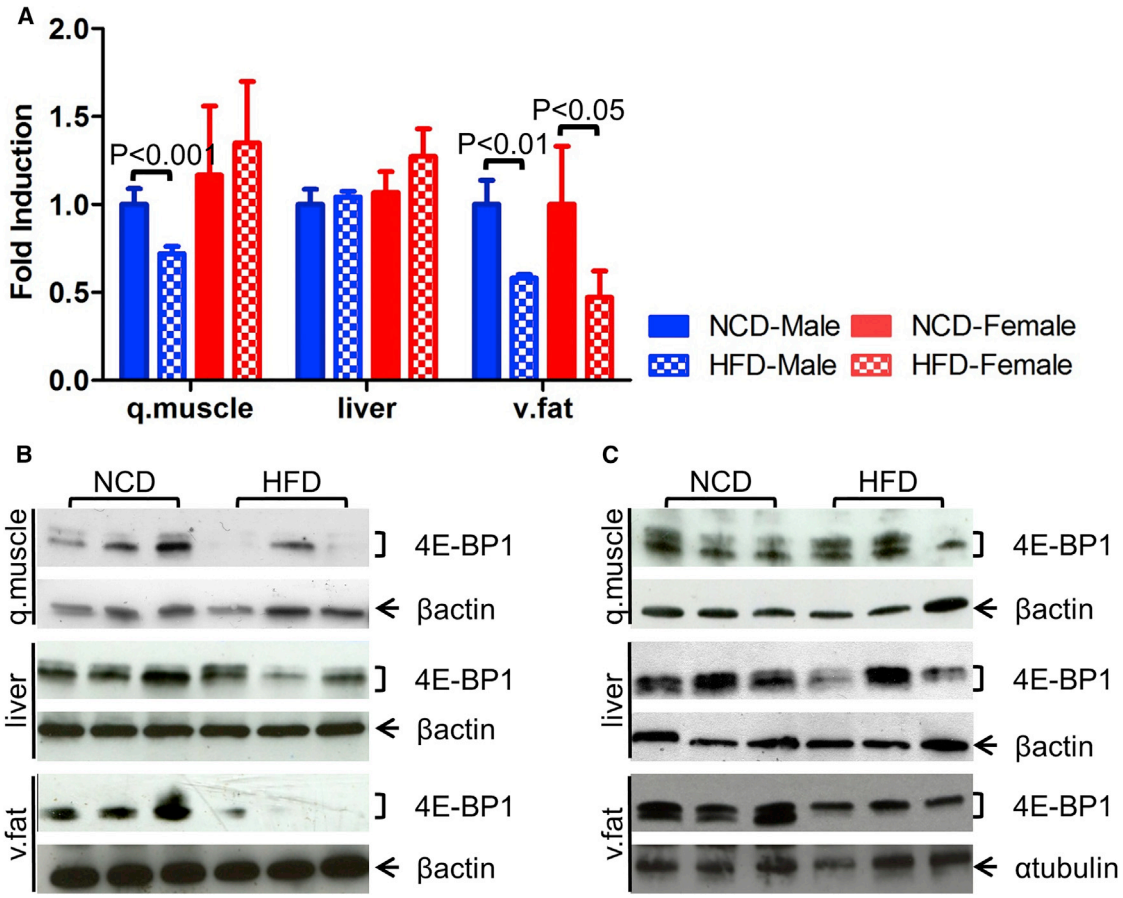


**Figure 2. Differential 4E-BP1 Expression in 6-Month-Old C57BL/6J Mice on a HFD**

(A) Real-time PCR analysis of *4E-BP1* mRNA expression in quadriceps muscle (q. muscle), liver, and visceral fat (v. fat) from normal diet-fed and HFD-fed male and female mice (n = 4). Fold induction was normalized to male normal diet-fed samples. Results are presented as mean ± SEM. p values were calculated by two-way ANOVA with Bonferroni post-tests to compare replicate means by row.

(B) Western blot of 4E-BP1 protein expression in quadriceps muscle, liver, and visceral fat from normal diet-fed or HFD-fed male mice.

(C) Western blot of 4E-BP1 protein expression in quadriceps muscle, liver, and visceral fat from normal diet-fed or HFD-fed female mice.

## Generation and Characterization of *4E-BP1* Transgenic Mice

Mice lacking 4E-BP1 and 4E-BP2 have increased obesity and insulin resistance on a HFD. Thus, we hypothesized that 4E-BPs are required to maintain adipose function in response to a HFD. To test this, we generated a transgenic mouse line with a conditional allele overexpressing *4EBP1*. The *4EBP1* transgenic allele (*Tg-4EBP1wt*) contains a human *4E-BP1* cDNA that was inserted under a hybrid cytomegalovirus enhancer and chicken $\beta$ *actin* promoter and preceded by a *loxP*-flanked GFP with a STOP cassette (Figure S3A). *CMV-Cre* transgenic mice, which express *Cre* during early embryogenesis, were bred with *Tg-4EBP1wt* mice to induce *4E-BP1* transgene allele expression in all tissues, including germ cells (Figure S3B). The transgenic 4E-BP1 protein competes with eIF4E associated with eIF4G from the translation initiation complex, as analyzed in a 7-methylguanosine 5′-triphosphate ($m^7$GTP) pull-down assay (Figures S3D and S3E). After germline transmission, the mice were bred to wild-type C57BL/6J to remove the *Cre* allele. We then backcrossed transgenic mice with whole-body *4E-BP1* overexpression to the C57BL/6J background for five generations to derive the *4EBP1wt-OE* mouse line for the assays described.

We found that 4E-BP1 was expressed at high levels in the skeletal muscle and liver of *4EBP1wt-OE* mice, with lower levels of expression in visceral fat (Figure S3B). It is also apparent that much of the expressed 4E-BP1 is in a phosphorylated state, likely as a result of mTORC1 activity (Figure S3C). *4EBP1wt-OE* mice are viable and fertile, and there is no obvious phenotype to distinguish them from control littermates (Figures S3F–S3H, S4A, and S4B). These mice also have normal glucose homeostasis, as examined in glucose tolerance and insulin challenge assays, even though male *4EBP1wt-OE* mice have a lower fasting glucose level at 6 months of age (Figures S4A and S4B).

## Reduced Adiposity in Male *4E-BP1* Transgenic Mice under HFD Feeding

We then challenged mice with HFD feeding to see whether *4EBP1wt-OE* mice are protected from diet-induced obesity.

After 16 weeks of HFD feeding, we found that male *4EBP1wt-OE* mice have a significant reduction both in body weight and adipose accumulation, whereas female *4EBP1-OE* mice develop a similar level of obesity as controls (Figures 3A and 3B; Figures S4C–S4G). Although male control mice gain 60% more weight than the NCD-fed control cohort, *4EBP1wt-OE* male mice only gain 19% more weight than their NCD-fed counterparts. Moreover, male *4EBP1wt-OE* mice also show less food intake than control counterparts on a HFD (Figure S4H). The difference in weight gain in HFD-fed *4EBP1wt-OE* and control male mice is mainly attributable to less fat accumulation (Figure S4C). Consistent with reduced obesity, male *4EBP1wt-OE* mice also have lower levels of serum leptin and triglycerides compared with control mice on a HFD (Figure 3C; Figure S4D).

Histological analysis of WT and *4EBP1wt-OE* adipose tissues clearly revealed a reduction in adiposity in male *4EBP1wt-OE* mice, with decreased white adipocyte accumulation and reduced adipocyte size (Figures S4E, S4F, and S5A). There was less accumulated white adipose tissue under the skin (subcutaneous fat) and also less white fat infiltration into brown adipose tissue; the latter is consistent with modestly increased UCP1 expression in brown adipose tissue of HFD-fed *4EBP1wt-OE* male mice (Figure S4G). Moreover, there was decreased macrophage accumulation, as stained by F4/80 antigen, in visceral fat of male *4EBP1wt-OE* mice, which correlated with a reduced level of IL-6 in serum of male *4EBP1wt-OE* mice (Figures S4I and S5A). Morbid obesity usually causes aberrant accumulation of triglycerides in the liver, which leads to hepatic steatosis and further impairs systemic fat metabolism. However, *4EBP1wt-OE* male mice, as determined by oil red O staining, clearly demonstrated a significant reduction of accumulated triglycerides in the liver on a HFD, indicative of improved systemic fat metabolism in these mice (Figure S5A).

## Maintenance of Insulin Sensitivity in Male 4E-BP1 Transgenic Mice under HFD Feeding

After 16 weeks of HFD feeding, both control male and female mice developed hyperglycemia. Fasting glucose was also elevated in *4EBP1wt-OE* male mice on HFD feeding but to a lesser extent than in non-transgenic control male mice (Figure 3D). Next we examined glucose homeostasis in *4EBP1wt-OE* mice. A glucose tolerance assay was performed to determine the ability of the mice to sense glucose elevation and secrete insulin as a means of promoting blood glucose uptake in peripheral tissues. Male *4EBP1wt-OE* mice display improved glucose homeostasis on a HFD, as demonstrated by improved glucose clearance relative to controls (Figure 3E). An insulin challenge assay was also performed to quantify systemic insulin resistance in mice on a HFD. The reduction of blood glucose levels was faster in male *4EBP1wt-OE* mice than in control mice over the course of the experiment (Figures S4K and S4L), with comparable insulin levels (Figure S4J). Furthermore, tissue of male *4EBP1wt-OE* mice maintained insulin-stimulated Akt phosphorylation (Figure 3F; Figure S5C–S5F).

Previously, we identified increased FGF21 signaling in a different line of 4E-BP1 transgenic mice that express in skeletal muscle a 4E-BP1 mutant allele resistant to mTORC1 regulation and demonstrated that these mice were also protected from HFD-induced obesity and insulin resistance (Tsai et al., 2015). The expression of FGF21 is also upregulated in male *4EBP1wt-OE* mice but, this time, in liver tissue (Figure S5B), suggesting that the levels of FGF21 and 4E-BP1 are positively associated. Another prospective mechanism in *4EBP1wt-OE* mice protected from HFD-induced metabolic dysfunction is through competing mTORC1 phosphorylating S6K1. However, we did not observe an alternation of phosphorylation status on either S6K1 or its target rpS6 under HFD feeding in multiple tissues of male *4EBP1wt-OE* mice (Figures S6A and S6B).

Among other mTORC1 targets examined in the HFD cohort, the phosphorylation of PRAS40, the proline-rich Akt substrate, by mTORC1 on Ser183 is increased in male mouse visceral fat upon HFD treatment (Figure S6C). Phosphorylation of PRAS40 at Ser183 by mTORC1 has been reported to suppress its ability to inhibit mTORC1 in vitro (Oshiro et al., 2007; Wang et al., 2008). The level of PRAS40 phosphorylation at Ser183 was reduced in fat tissue of mice overexpressing 4E-BP1, although the trend did not reach significance (Figure S6D). The repression of PRAS40 phosphorylation in male *4EBP1wt-OE* mice is more profound in visceral fat during aging, as discussed in more detail below (Figure S9A). Previously, DEPTOR, another mTOR-interacting protein, has been shown to positively regulate adipogenesis in vitro, and its expression is associated with obesity in vivo (Laplante et al., 2012). The changes of DEPTOR expression were not evident in HFD-treated mouse tissues (Figure S6E), but there is a slight induction of DEPTOR expression in the visceral fat of male *4EBP1wt-OE* mice (Figure S6F). In the context of overnutrition, male *4EBP1wt-OE* mice have improved glucose tolerance and increased insulin sensitivity on a HFD. Mechanistically, the improved metabolic function might occur through induction of FGF21 production in male *4EBP1wt-OE* mice.

## Tissue-Specific Induction of *4E-BP1* in Adipose or Skeletal Muscle Does Not Provide Metabolic Protection in Mice on a HFD

Because 4E-BP1 expression is predominately reduced in adipose tissue and skeletal muscle upon HFD, we crossed *Tg-4EBP1* mice with either *Fabp4-Cre* (*Tg-4EBP1wt*;*Fabp4-Cre*, referred to as *Tg-4EBP1wt-fat*) or *Ckmm-Cre* (*Tg-4EBP1wt*;*Ckmm-Cre*, referred to as *Tg-4EBP1wt-muscle*) mice to remove the *loxP*-flanked GFP-STOP codon cassette and promote *4E-BP1* transgene allele expression in mouse adipose tissue or skeletal muscle, respectively (Figures S7A and S7B). This approach was designed to determine whether 4E-BP1 activity is required to achieve protection from a HFD challenge. Both transgenic mouse lines were backcrossed to the C57BL/6J background for five generations prior to their characterization.

Both *Tg-4EBP1wt-fat* and *Tg-4EBP1wt-muscle* mice have comparable body weight, adiposity, lean body mass, and glucose metabolism in comparison with control littermates (Figure 4; Figures S7C–S7E). We subjected both transgenic mouse lines to a HFD challenge starting at 8 weeks of age and monitored their weight and glucose metabolism during the course of 16 weeks. Neither *Tg-4EBP1wt-fat* nor *Tg-4EBP1wt-muscle* mice of either gender show any metabolic protection from HFD-induced obesity and insulin resistance (Figure 4; Figures

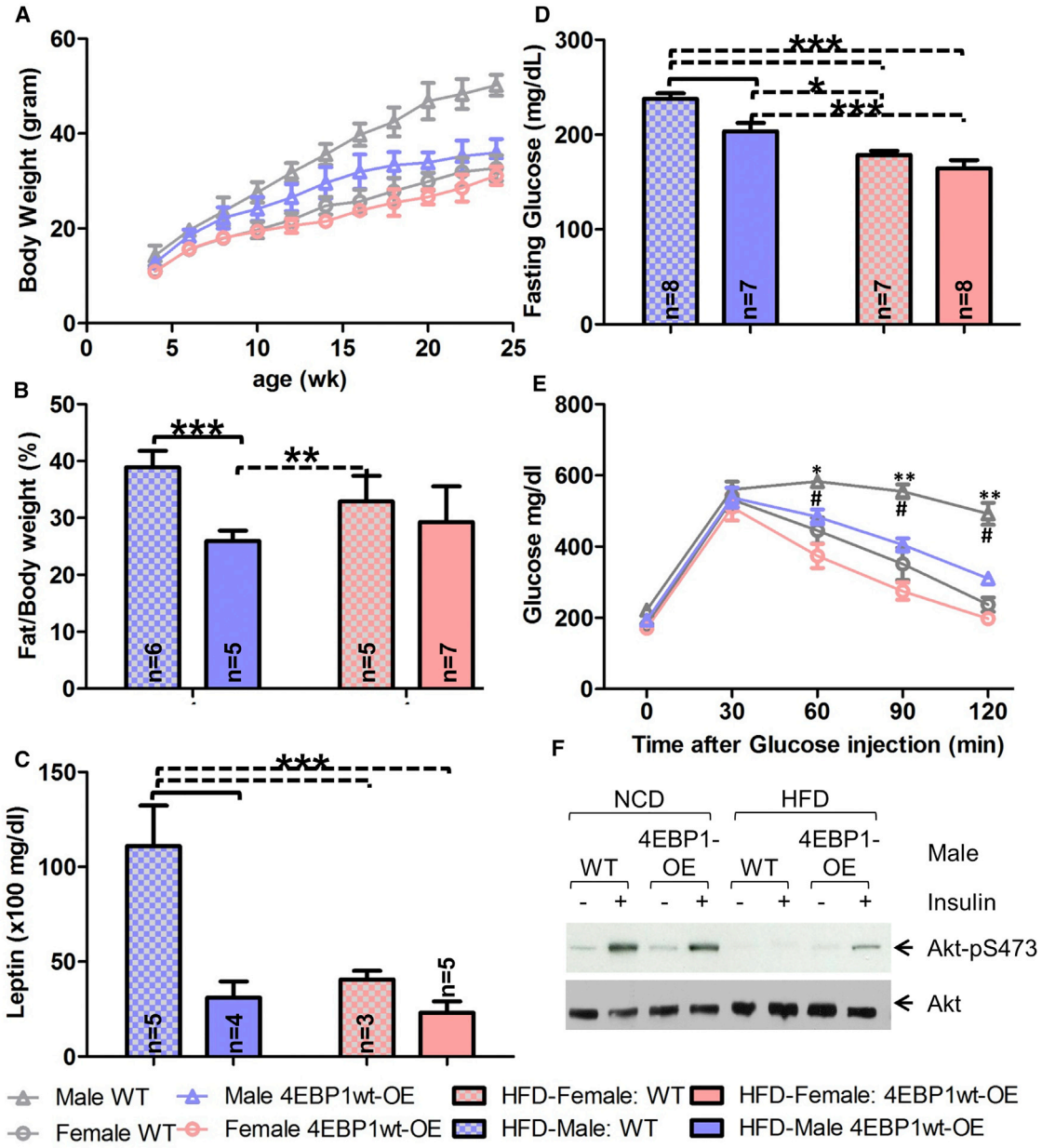


**Figure 3. Male *4EBP1-OE* Transgenic Mice Are Protected from Diet-Induced Obesity and Maintain Insulin Sensitivity**

(A) Body weight measurement in *4EBP1-OE* transgenic and wild-type mice on a HFD (n = 7–9). $p < 0.001$ (WT versus *4EBP1-OE*: males started at week 10). $p < 0.001$ (males versus females: WT started at week 8). $p < 0.001$ (males versus females: *4EBP1-OE* started at 8 weeks]. Male *4EBP1-OE* versus female WT, $p < 0.01$ at weeks 8–14, $p < 0.001$ at weeks 16–18, and $p < 0.05$ at week 20. $p < 0.001$ (male WT versus female *4EBP1-OE* started at week 6).

(B) Adiposity measurement in 6-month-old *4EBP1-OE* transgenic and wild-type mice on a HFD.

(C). Plasma leptin measurement in *4EBP1-OE* transgenic and wild-type mice on a HFD at 6 months of age.

(D) Plasma glucose measurement in 6 hr-fasting *4EBP1-OE* transgenic and wild-type mice on a HFD at 6 months of age.

(E) Glucose tolerance assay in 6 hr-fasting *4EBP1-OE* transgenic and wild-type mice on a HFD at 6 months of age (n = 9). *$p < 0.05$, **$p < 0.001$ (*WT* versus *4EBP1wt-OE*: male). #$p < 0.001$ (male versus female: WT).

(F) Western blot of phosphorylation of AKT1 at Ser473 and total AKT1 protein expression in visceral fat of *4EBP1-OE* transgenic and wild-type male mice before (–) or after (+) insulin stimulation on a normal chow diet or HFD at 6 months of age.

All graphs are plotted as mean ± SEM of the number of mice used in each analysis. The numbers of samples analyzed are indicated. p Values were calculated by two-way ANOVA in (B–D) and two-way ANOVA for repeated measures in (A) and (E), with Bonferroni post-tests to compare replicate means by row. For simplicity, in (B–D), the p values of the cross-comparison from the other groups was labeled as follows: *$p < 0.05$, **$p < 0.01$, ***$p < 0.001$.

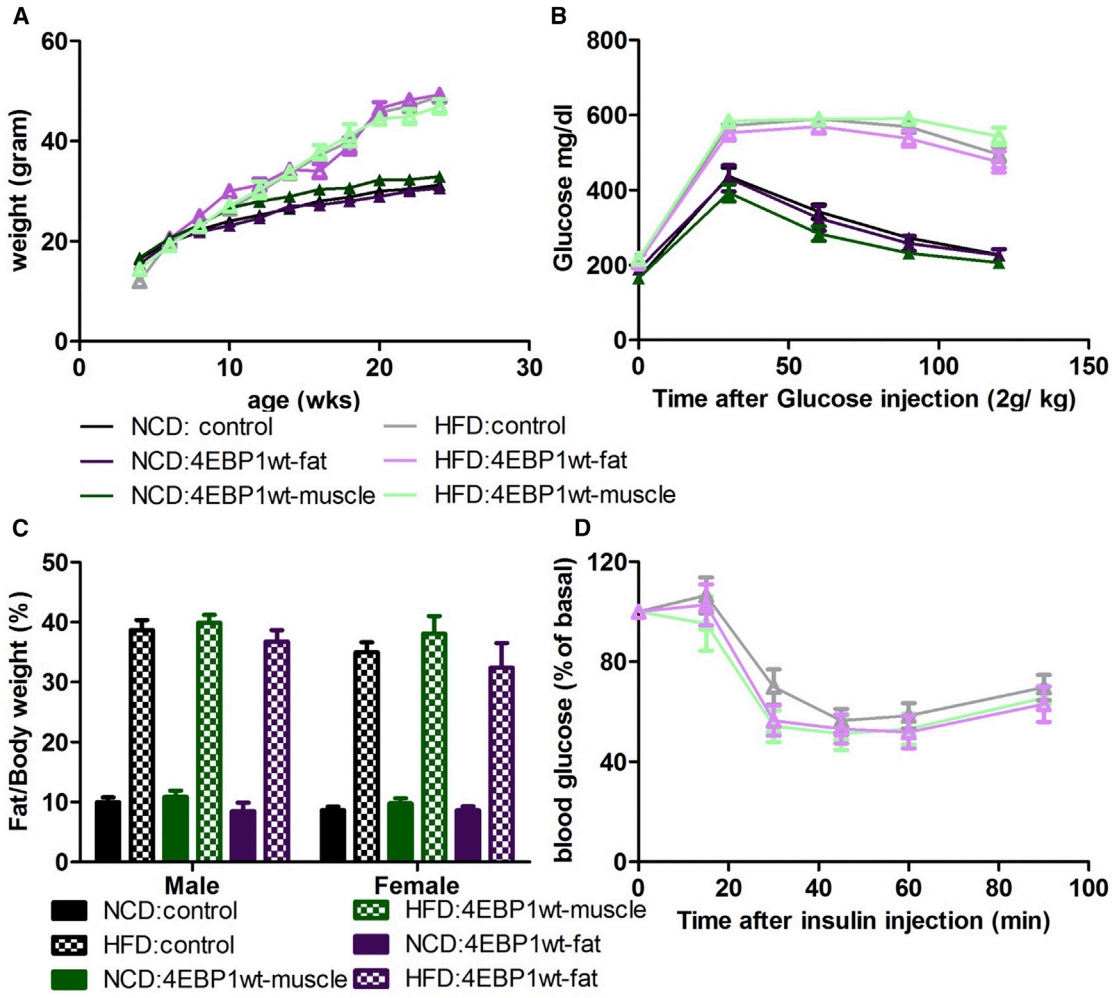


**Figure 4. Assessment of Metabolic Parameters in *4E-BP1* Double-Transgenic Male Mice**

(A) Body weight measurement in *Tg-4EBP1wt-fat* and *Tg-4EBp1wt-muscle* male mice on a normal chow diet and HFD (n = 8–16). $p < 0.001$ (NCD versus HFD: males started at 10 weeks).

(B) Glucose tolerance assay in 6 hr-fasting *Tg-4EBP1wt-fat* and *Tg-4EBp1wt-muscle* male mice on a normal chow diet and HFD at 6 months of age (n = 8–16). $p < 0.001$ (NCD versus HFD in all genetic group comparisons: males started at the 30-min time point).

(C) Fat mass measurement normalized with body weight in *Tg-4EBP1wt-fat* and *Tg-4EBp1wt-muscle* mice on a normal chow diet and HFD at 6 months of age (n = 8–16). $p < 0.001$ (NCD versus HFD in all genetic and gender group comparisons).

(D) Insulin challenge assay in 6 hr-fasting *Tg-4EBP1wt-fat* and *Tg-4EBp1wt-muscle* male mice on a HFD at 6 months of age (n = 8–16).

All graphs are plotted as mean ± SEM of the number of mice used in each analysis. The number of samples analyzed is indicated. p Values were calculated by two-way ANOVA (C) and two-way ANOVA for repeated measures (B) and (D) with Bonferroni post-tests to compare replicate means by row.

S7C–S7F). The *4E-BP1* transgenic allele encodes a wild-type 4E-BP1 protein that retains regulation by mTORC1-dependent phosphorylation. Thus, increased mTORC1 signaling on a HFD may partially or fully inactivate transgenic overexpressed 4E-BP1 protein, preventing any observed metabolic protection in these transgenic mice. Consistent with this prediction, we observed an increase in 4E-BP1 phosphorylation in both transgenic mouse tissues (Figures S7G and S7H). These findings suggest that the protection conferred by whole-body overexpression of 4E-BP1 cannot be recapitulated by overexpression specifically in muscle or fat. The benefits must derive from expression in another tissue or a combination of tissues.

## Male *4E-BP1* Transgenic Mice Are Protected from Aging-Induced Obesity and Metabolic Rate Decline

Both male and female *4EBP1wt-OE* mice were leaner than controls during aging, but the difference was more pronounced in male transgenic mice, which showed significantly reduced adiposity starting at approximately 1 year of age (Figures 5A and 5B; Figure S8A). Male *4EBP1wt-OE* mice also have significantly reduced levels of serum leptin and triglycerides along with reduced adiposity (Figures S8B and S8C). These differences are not the result of altered food intake or activity (Figures S8D and S8E). There is also no change in respiratory exchange ratio in *4EBP1wt-OE* mice (Figure S8F). Nevertheless, male

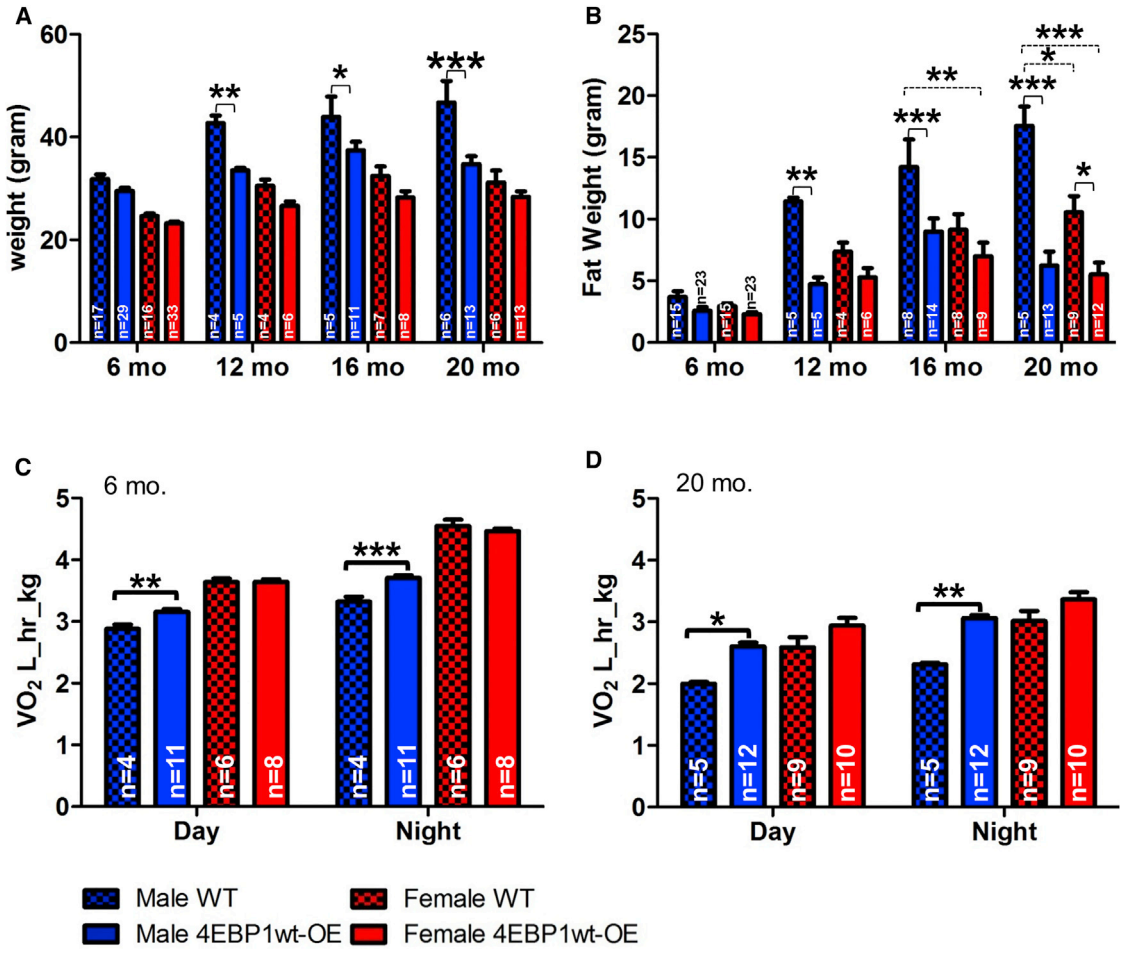


**Figure 5. Metabolic Parameters of Aging *4EBP1-OE* Transgenic and Wild-Type Mice on a Normal Chow Diet**

(A) Body weight measurement in *4EBP1-OE* transgenic and wild-type mice on a normal chow diet. $p < 0.001$ (males versus females: WT). $p < 0.001$ (males versus females: *4EBP1-OE*). Male *4EBP1-OE* versus female WT, $p < 0.01$ at 6 months. $p < 0.001$ (male WT versus female *4EBP1-OE*).

(B) Fat weight measurement in *4EBP1-OE* transgenic and wild-type mice on a normal chow diet during aging.

(C) Oxygen consumption in *4EBP1-OE* transgenic and wild-type mice on a normal chow diet at 6 months of age. $p < 0.001$ (males versus females: WT), $p < 0.001$ (male WT versus female *4EBP1-OE*), $p < 0.001$ (male *4EBP1-OE* versus female), $p < 0.001$ (male WT versus female *4EBP1-OE*).

(D) Oxygen consumption in *4EBP1-OE* transgenic and wild-type mice on a normal chow diet at 20 months of age. $p < 0.01$ (males versus females: WT), $p < 0.001$ (male WT versus female *4EBP1-OE*).

All graphs are plotted as mean ± SEM of the number of mice used in each analysis. The numbers of samples analyzed are indicated. p Values were calculated by two-way ANOVA with Bonferroni post-tests to compare replicate means by row. *$p < 0.05$, **$p < 0.01$, ***$p < 0.001$.

*4EBP1wt-OE* mice have an increased metabolic rate (Figures 5C and 5D) that is evident as early as 6 months of age, when their body weight is comparable with control littermates (Figure 5A). Consistent with the HFD cohort, no difference was observed in S6K1 phosphorylation or its downstream target rpS6 (Figures S8G and S8H). The protein stability of IRS1, insulin receptor substrate 1, is affected by serine phosphorylation by either S6K1 at Ser307 or mTORC1 at Ser636/639 and has been proposed to lead to insulin resistance (Copps and White, 2012; Um et al., 2006). Consistent with the lack of alteration of S6K1 phosphorylation, we also failed to observe any significant changes in serine phosphorylation of IRS1 or IRS1 stability (Figure S8I; data not shown). Moreover, there is no reduction of global translation in *4EBP1wt-OE* mouse tissues (Figure S8J).

Mice develop a comparable level of obesity during the course of a 22-month aging study and a 4-month HFD feeding study (Figure S8K). We found that there is a trend toward reduction in PRAS40 phosphorylation seen in HFD-fed *4EBP1wt-OE* male visceral fat (Figure S6D), and the reduction in PRAS40 phosphorylation is more profound during aging in the same tissue (Figure S9A).

We also observed a higher level of FGF21 (Figure S9B) in *4EBP1wt-OE* male mouse serum, likely associated with protection of brown adipose during aging (Figure S9C) and higher levels of *Ucp1* and *Pgc1α* expression in brown adipose tissue of aged *4EBP1wt-OE* male mice (Figure S9E). There is a slight upregulation in mRNA levels of genes involved in thermogenesis in subcutaneous white adipose tissues of *4EBP1wt-OE* male mice

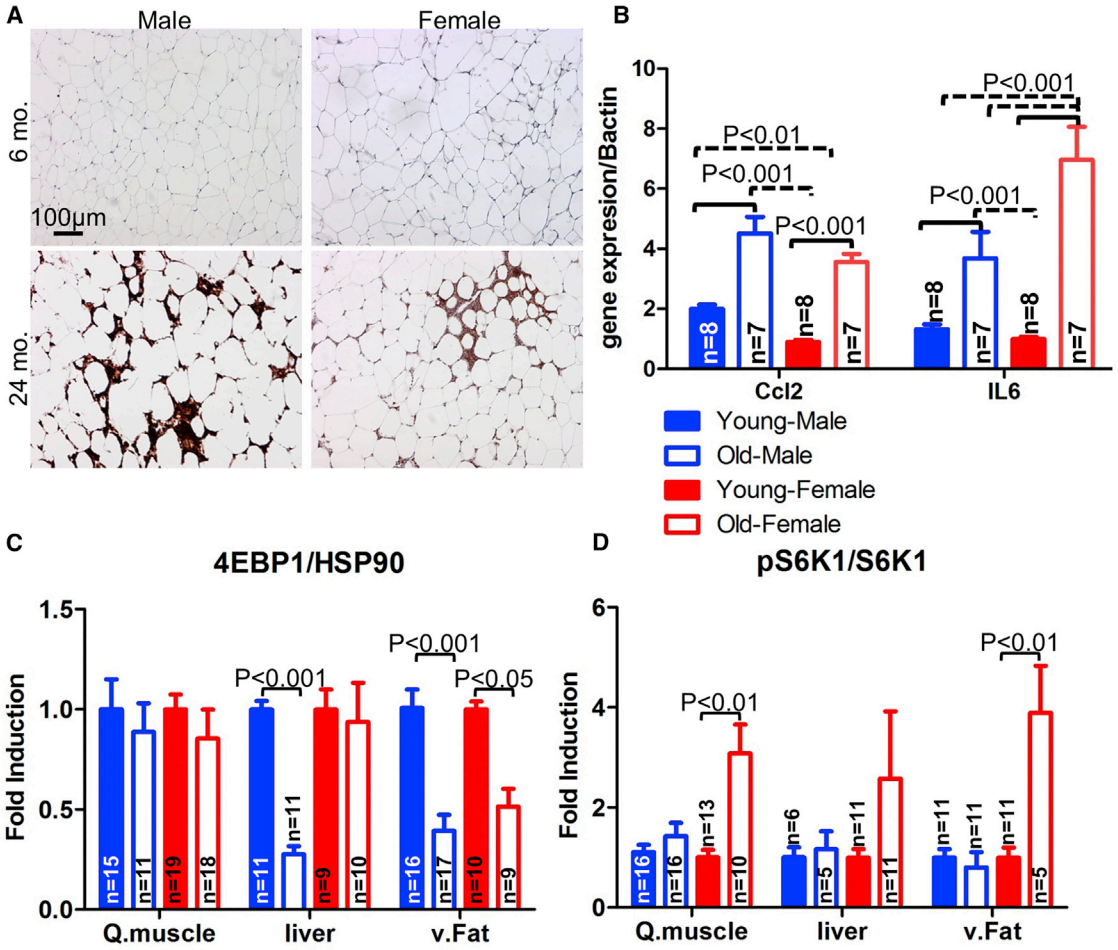


**Figure 6. Gender Dimorphism in Expression of 4E-BP1 and Activity of S6K1 in Aging C57BL/6J Mice**

(A) Macrophage infiltration in visceral fat stained by F4/80 IHC from 6-month-old or 24-month-old wild-type male and female mice (n = 4 for the 6-month-old cohort and n = 7 for the 24-month-old cohort).

(B) Real-time PCR analysis of proinflammatory gene expression in visceral fat from 6-month-old or 24-month-old wild-type male or female mice (n = 8 for the 6-month-old cohort and n = 7 for the 24-month-old cohort). Fold induction was normalized to 6-month-old female samples.

(C) Quantification of the western blot of 4E-BP1expression normalized with the housekeeping gene HSP90 relative to 6-month-old samples.

(D) Quantification of the western blot of phosphorylated S6K1 at Thr389 normalized with total S6K1 expression relative to 6-month-old samples.

Young mouse cohorts were from 6-month-old mice, and old mouse cohorts were from 24-month-old mice. All graphs are plotted as mean ± SEM of the number of mice used in each analysis. p Values were calculated by two-way ANOVA with Bonferroni post-tests to compare replicate means by row.

(Figure S9D). Moreover, male *4EBP1wt-OE* mice have reduced muscle damage during aging, including lower numbers of centralized, vacuolated fibers, and decreased intramuscular fatty acid accumulation (Figures S9F and S9G).

In a further analysis of aging tissues, we found a similar negative correlation of inflammation and 4E-BP1 expression as in the HFD cohort (Figures 1E, 1F, and 2). The increased macrophage infiltration and induced pro-inflammatory cytokine gene expression (Figures 6A and 6B) is associated with reduced 4E-BP1 expression in visceral fat of both aging male and female mice (Figure 6C). Consistent with this notion, whole-body overexpression of 4E-BP1 protected both males and females from aging-induced obesity (Figure 5B). Moreover, there is a gender difference in the expression of the mTORC1 targets S6K1 and 4E-BP1 in aging tissues. 4E-BP1 is selectively reduced in male liver and visceral fat, whereas phosphorylation of S6K1, or its target S6, is exclusively upregulated in aging female tissues (Figures 6C and 6D; Figure S10). The distinct expression pattern of 4E-BP1 and S6K1 in aging mouse tissues could be the reason why only female *s6k1* knockout mice have a lifespan extension (Selman et al., 2009) and male *4EBP1wt-OE* mice are protected from aging-induced metabolic decline.

## DISCUSSION

Here, we report a gender-dependent divergence in 4E-BP1 expression and its effect on metabolic regulation in response to different diets. With a HFD challenge, 4E-BP1 expression is significantly reduced in male skeletal muscle and adipose tissue. Male and female mice develop a similar level of obesity on a

HFD, but male mice have aggravated and deregulated lipid and glucose metabolism. Furthermore, increased expression of 4E-BP1 rescues male mice from diet-induced obesity and insulin resistance, whereas 4E-BP1 overexpression does not provide beneficial protection to HFD-fed female mice.

In the context of aging, we found that expression of 4E-BP1 is selectively downregulated in aging male mouse liver and adipose tissue. Overexpression of 4E-BP1 protects male mice from aging-induced obesity and increases energy expenditure. Conversely, we observed enhanced upregulation of S6K1 activity in aging female liver, skeletal muscle, and adipose tissues. The sexual-dimorphic regulation of two mTORC1 targets, S6K1 and 4E-BP1, correlates with the enhanced lifespan of female *s6k1* knockout mice and improved metabolic homeostasis in male *4EBP1wt-OE* mice during aging. Recently, Baar et al. (2016) reported that there is variation in mTORC1 signaling during aging of C57BL/6J mice. S6K1 was upregulated in adipose tissues of fasted male and female mice and skeletal muscle tissues of male mice, and there was no difference in 4E-BP1 expression. The differences between these two studies in the assessment of mTORC1 signaling from aging tissues could be due to the nutrition status of the mice at the time they were harvested because the mTOR pathway is highly sensitive to calorie intake. We harvested mice in the morning after they had ad libitum access to food during the evening, whereas Baar et al. (2016) harvested mice after overnight fasting. Further studies will be required to explain how nutrition and aging intersect to influence mTOR signaling. Adipose tissue plays a central role in the management of whole-body energy expenditure, regulating both glucose homeostasis and insulin sensitivity (Blüher et al., 2003). Altered mTORC1 signaling is implicated in obese human and animal adipose tissues. Specific deletion of mTORC1 in adipose tissue or whole-body inactivation of its downstream mediator, S6K1, in mice leads to reduced adiposity and increased metabolic rate. Both mice were also protected from HFD-induced obesity and insulin resistance (Polak et al., 2008; Um et al., 2004). Conversely, whole-body inactivation of 4E-BP1 and 4E-BP2, which are negatively regulated by mTORC1, results in increased adiposity and sensitivity to HFD-induced metabolic dysfunction (Le Bacquer et al., 2007). Previous studies did not examine the mTORC1 pathway for gender-specific effects.

Here we have demonstrated that mTORC1 signaling behaves differently in male and female mice via 4E-BP1. A HFD preferentially suppresses 4E-BP1 expression in male adipose tissues, which is correlated with increased adiposity and adipokine secretion. Overexpression of 4E-BP1 reverses these defects. The molecular mechanism underlying how 4E-BP1 expression is differentially regulated by gender is not clear. One likely explanation involves sexual dimorphic regulation of inflammation, which, in turn, regulates 4E-BP1 expression.

Gender differences in the intrinsic characteristics of adipose tissue and the subsequent response to overnutrition have been reported (Macotela et al., 2009; Nickelson et al., 2012; Pettersson et al., 2012). For example, despite the higher level of body fat, female humans and rodents are more insulin-sensitive than males. During overnutrition in humans and rodents, male subjects have increased adipokine secretion, which contributes to inflammation and early abnormalities of glucose metabolism. The mechanism underlying this phenomenon is in part due to the action of estrogen and testosterone. For example, females after menopause exhibit higher risk for the development of insulin resistance, and castrated male rodents are more insulin-sensitive (Mauvais-Jarvis et al., 2013). Hormonal regulation could also contribute to sex-specific regulation of 4E-BP1 expression.

It remains unclear in which tissues 4E-BP1 is regulated in a gender-specific manner during overnutrition and aging and where overexpression of 4E-BP1 rescues metabolic dysfunction in males. Recently, we reported that transgenic expression of activated, mTORC1-non-responsive 4E-BP1 in skeletal muscle, but not adipose tissue, protects mice of both genders from high fat diet-induced metabolic dysfunction (Tsai et al., 2015). Because activated 4E-BP1 is refractory to the elevated mTORC1 signaling associated with exposure to a high-fat diet, one possibility is that the primary benefits of 4E-BP1 activation are in skeletal muscle. A small increase in 4E-BP1 activity when the wild-type protein is overexpressed might only be sufficient to suppress defects associated with loss of 4E-BP1 in male mice during a high-fat diet or aging. Higher skeletal muscle activity in the 4E-BP1 mutant may increase metabolic protection in both genders under the same challenges. Alternatively, the phenotypes associated with whole-body overexpression of wild-type 4E-BP1 may derive from enhanced activity in other tissues. Further studies will be required to resolve this issue.

Our results demonstrate that 4E-BP1 expression in adipose and skeletal muscle tissue is a key determining factor in the gender dimorphism of fat metabolism and insulin sensitivity. In addition, they provide genetic evidence for gender differences in the response to overexpression of 4E-BP1 in obesity. Hence, our findings have important implications for the treatment of metabolic syndrome, obesity, and T2D because gender differences in the response to drugs targeting the mTORC1 pathway may exist in humans.

## EXPERIMENTAL PROCEDURES

### Generation of *4E-BP1* Transgenic Mice and Animals Studies

Human *4E-BP1* cDNA was placed downstream of a *loxP*-GFP-3xstop-*loxP* cassette under the control of a chicken *β-actin* promoter. The GFP-STOP cassette prevents expression of the *4E-BP1* transgenic allele. Transgenic mice were then crossed with mice expressing CRE under the control of a human cytomegalovirus minimal promoter (*CMV-Cre*) to induce whole-body *4E-BP1* transgene expression, fatty acid-binding protein 4 promoter (Fabp4-Cre) to induce adipose tissue *4E-BP1* transgene expression, or the muscle creatine kinase promoter (*Ckmm-Cre*) to induce skeletal muscle tissue 4E-BP1 transgene expression. All mice in this study were five generations into the C57BL6/J background. In the high-fat diet-induced type II diabetes study, mice at 8 weeks of age were placed on either a standard laboratory rodent chow (#2018, Harlan Teklad) or a high-fat diet (D12492, Research Diets), as indicated, and monitored for 24 weeks. Mice were handled in accordance with, and all in vivo studies were approved by, the Institutional Animal Care and Use Committee (A10093) at the Buck Institute for Research on Aging.

### Histological Analysis

Tissue samples were either fixed in 4% paraformaldehyde solution in PBS before being embedded in paraffin or directly mounted in optimal cutting temperature compound (OCT) before being stored at −80°C. Morphology was examined in H&E-stained sections. The size of adipose cells was quantified in ImageJ. Results are shown as a mean ± SEM of three to six independent animals. The oil red O staining was performed in OCT-mounted liver sections and

flash-frozen muscle tissue sections. 10-μm-thick sections were cut and allowed to dry for 10 min. After the air-drying process, the slides were rinsed for a short time in distilled water and stained in 300 mg/dl oil red O solution in isopropanol for 15 min. The slides were then transferred to 60% isopropanol to clean the background and resin in distilled water and processed for hematoxylin counterstaining. Macrophage infiltration of white adipose tissue was stained using monoclonal F4/80 antibody (Invitrogen) on paraffin sections.

### Blood Lipid, Glucose, and Hormone Analyses

Mouse blood was collected using the submandibular pouch technique. Serum was separated using serum separator tubes (BD 365956). The analyses of triglyceride, FGF21, insulin, and leptin levels were performed in sera collected from mice that were fasted for 6 hr. The IL-6 assay was performed on serum from non-fasted mice. The triglyceride test (2100-430) was purchased from Stanbio, the analysis of FGF21 (MF2100) and IL-6 (M6000B) ELISA was purchased from R&D Systems, the analysis of insulin (NR 10-1247-01) ELISA was purchased from Mercodia, and all were performed following the manufacturer's instructions. The leptin tests were done in the Diabetes, Endocrinology, and Metabolism Hormone Assay and Analytical Services Core at Vanderbilt University.

### Glucose and Insulin Tolerance Assays

Glucose and insulin tolerance tests were performed on 6-month-old mice that were fasted for 6 hr. Glucose concentrations were determined with an Accu-Chek advantage glucometer (Roche) in blood collected from the tail vein at indicated time points. Insulin (0.75 U/kg for HFD group mice and 0.375 U/kg for NCD group mice) or glucose (2 g/kg) was injected intraperitoneally into mice. Insulin was Humulin R (U-100) from Lilly.

### RNA Analyses

Total RNA was extracted from tissue using Trizol (Life Technologies) following the manufacturer's instructions (n = 4 for each group, 6-month-old mice). 2 μg of total RNA was reverse-transcribed into cDNA by using the Superscript III reverse transcription kit (Invitrogen). Real-time PCR was performed in a Roche 480 iCycler PCR machine. Reactions were performed in triplicate, and relative amounts of cDNA were normalized to *Cyclophilin A* (*Ppia*). Primer sequences were as follows: *4E-BP1* forward, CTAGCCCTACCAGCGATGAG; *4E-BP1* reverse, CCTGGTATGAGGCCTGAATG; *Ppia* forward, GACCAAACA CAAACGGTTCC; *Ppia* reverse, CATGCCTTCTTTCACCTTCC; *IL-6* forward, CCGGAGAGGAGACTTCACAG; *IL-6* reverse, TTCTGCAAGTGCATCATCGT; *Ccl-2* forward, CCCAATGAGTAGGCTGGAGA; *Ccl-2* reverse, TCTGGACC CATTCCTTCTTG. *Ucp-1* forward, GCCTGGCAGATATCATCACC; *Ucp-1* reverse, CAGACCGCTGTACAGTTTCG; *Pgc-1α* forward, AACCACACCCA CAGGATCAGA; *Pgc-1α* reverse, TCTTCGCTTTATTGCTCCATGA; *Cidea* forward, CTCGGCTGTCTCAATGTCAA; *Cidea* reverse, GGAACTGTCCCGT CATCTGT; *Dio2* forward, GCTGTGTCTGGAACAGCTTC; *Dio2* reverse, TGAACCAAAGTTGACCACCA; *Prdm16* forward, GAGCAGCTGAGGAAG CATTT; *Prdm16* reverse, GCGTGGAGAGGAGTGTCTTC; *Stat6* forward, CTGCCTAACTCAGCCTGTGG; *Stat6* reverse, CCTGATTGCCCATAAGGAGA.

### Protein Isolation and Immunoblotting Studies

Tissues were homogenized in cold SDS lysis buffer (50 mM Tris [pH 7.5], 70 mM urea, 250 mM sucrose, and 2% SDS) with protease inhibitor cocktail (Roche, 04693124001) and phosphatase inhibitor cocktails II and III (Sigma, P5726 and P0044). Total proteins were separated in 4%–12% Invitrogen BT precast gel (NP0315) or any KD Bio-Rad TGX precast gel (456-9033) and transferred to nitrocellulose membranes. Antibodies were from Cell Signaling Technology (α-4E-BP1 [#9252], α-phospho-4EBP1 Ser65 [#9451], α-phospho-4EBP1 Thr37/46 [#9459], α-S6 [#2217], α-phospho-S6 Ser235/236 [#2211], α-AKT1 [#4691], α-phospho-AKT Ser473 [#4060], α-JNK [#9258], α-phospho-JNK Thr183/Tyr185 [#9251], α-eIF4E [#2067], α-eIF4G [#2469], α-S6K1 [#2708], α-phospho-S6K1 Thr389 [#9234], α-PRAS40 [#2691], α-phospho-PRAS40 Ser183 [#5936], α-IRS1 [#3015], α-phospho-IRS1 Ser636/639 [#2388], α-HSP90 [#4877], α-αtubulin [#3873], and α-β ACTIN [#4967]), Abcam (α-FGF21 [ab171941] and α-UCP1 [ab23841]), and EMD Millipore (α-DEPTOR, ABS222).

### Indirect Calorimetric Studies

Oxygen consumption, $CO_2$ production, home activity, and food were measured by open-flow respirometry (Sable Systems).

### Statistics

Unless otherwise stated, all results are expressed as mean ± SEM of n observations. Statistical differences between the means were assessed by two-way ANOVA, and all glucose tolerance assays and insulin challenge assays were analyzed by two-way ANOVA for repeated measures. Bonferroni post-tests were used to compare replicate means by row.

## SUPPLEMENTAL INFORMATION

Supplemental Information includes ten figures and can be found with this article online at http://dx.doi.org/10.1016/j.celrep.2016.07.029.

## AUTHOR CONTRIBUTIONS

All experiments were designed and conceived by S.Y.T., A.R.L., and B.K.K. The experiments were performed by S.Y.T., A.A.R., S.G.D., J.M.S., E.C.A., and T.D.A. Data analysis was done by S.Y.T. The manuscript was written by S.Y.T., A.R.L., and B.K.K.

## ACKNOWLEDGMENTS

This study was supported by NIH Grants R01AG033373 and R01AG035336 (to B.K.K.) and R01 AG033082 (to A.R.L.). B.K.K. is also an Ellison Medical Foundation Senior Scholar in Aging. The graphical abstract was contributed by Wan-Lin Lo.

Received: September 17, 2015
Revised: June 9, 2016
Accepted: July 13, 2016
Published: August 4, 2016

## REFERENCES

Baar, E.L., Carbajal, K.A., Ong, I.M., and Lamming, D.W. (2016). Sex- and tissue-specific changes in mTOR signaling with age in C57BL/6J mice. Aging Cell *15*, 155–166.

Bloor, I.D., and Symonds, M.E. (2014). Sexual dimorphism in white and brown adipose tissue with obesity and inflammation. Horm. Behav. *66*, 95–103.

Blüher, M., Kahn, B.B., and Kahn, C.R. (2003). Extended longevity in mice lacking the insulin receptor in adipose tissue. Science *299*, 572–574.

Brown, L.M., Gent, L., Davis, K., and Clegg, D.J. (2010). Metabolic impact of sex hormones on obesity. Brain Res. *1350*, 77–85.

Carnethon, M.R., De Chavez, P.J., Biggs, M.L., Lewis, C.E., Pankow, J.S., Bertoni, A.G., Golden, S.H., Liu, K., Mukamal, K.J., Campbell-Jenkins, B., and Dyer, A.R. (2012). Association of weight status with mortality in adults with incident diabetes. JAMA *308*, 581–590.

Copps, K.D., and White, M.F. (2012). Regulation of insulin sensitivity by serine/threonine phosphorylation of insulin receptor substrate proteins IRS1 and IRS2. Diabetologia *55*, 2565–2582.

Cornu, M., Albert, V., and Hall, M.N. (2013). mTOR in aging, metabolism, and cancer. Curr. Opin. Genet. Dev. *23*, 53–62.

Cowie, C.C., Rust, K.F., Byrd-Holt, D.D., Gregg, E.W., Ford, E.S., Geiss, L.S., Bainbridge, K.E., and Fradkin, J.E. (2010). Prevalence of diabetes and high risk for diabetes using A1C criteria in the U.S. population in 1988-2006. Diabetes Care *33*, 562–568.

Dazert, E., and Hall, M.N. (2011). mTOR signaling in disease. Curr. Opin. Cell Biol. *23*, 744–755.

Elbein, S.C., Gamazon, E.R., Das, S.K., Rasouli, N., Kern, P.A., and Cox, N.J. (2012). Genetic risk factors for type 2 diabetes: a trans-regulatory genetic architecture? Am. J. Hum. Genet. *91*, 466–477.

Gödel, M., Hartleben, B., Herbach, N., Liu, S., Zschiedrich, S., Lu, S., Debreczeni-Mór, A., Lindenmeyer, M.T., Rastaldi, M.P., Hartleben, G., et al. (2011). Role of mTOR in podocyte function and diabetic nephropathy in humans and mice. J. Clin. Invest. *121*, 2197–2209.

Grove, K.L., Fried, S.K., Greenberg, A.S., Xiao, X.Q., and Clegg, D.J. (2010). A microarray analysis of sexual dimorphism of adipose tissues in high-fat-diet-induced obese mice. Int. J. Obes. *34*, 989–1000.

Inoki, K., Mori, H., Wang, J., Suzuki, T., Hong, S., Yoshida, S., Blattner, S.M., Ikenoue, T., Rüegg, M.A., Hall, M.N., et al. (2011). mTORC1 activation in podocytes is a critical step in the development of diabetic nephropathy in mice. J. Clin. Invest. *121*, 2181–2196.

Laplante, M., and Sabatini, D.M. (2012). mTOR signaling in growth control and disease. Cell *149*, 274–293.

Laplante, M., Horvat, S., Festuccia, W.T., Birsoy, K., Prevorsek, Z., Efeyan, A., and Sabatini, D.M. (2012). DEPTOR cell-autonomously promotes adipogenesis, and its expression is associated with obesity. Cell Metab. *16*, 202–212.

Le Bacquer, O., Petroulakis, E., Paglialunga, S., Poulin, F., Richard, D., Cianflone, K., and Sonenberg, N. (2007). Elevated sensitivity to diet-induced obesity and insulin resistance in mice lacking 4E-BP1 and 4E-BP2. J. Clin. Invest. *117*, 387–396.

Lyssenko, V., and Laakso, M. (2013). Genetic screening for the risk of type 2 diabetes: worthless or valuable? Diabetes Care *36* (*Suppl 2*), S120–S126.

Macotela, Y., Boucher, J., Tran, T.T., and Kahn, C.R. (2009). Sex and depot differences in adipocyte insulin sensitivity and glucose metabolism. Diabetes *58*, 803–812.

Mauvais-Jarvis, F., Clegg, D.J., and Hevener, A.L. (2013). The role of estrogens in control of energy balance and glucose homeostasis. Endocr. Rev. *34*, 309–338.

Morris, A.P., Voight, B.F., Teslovich, T.M., Ferreira, T., Segrè, A.V., Steinthorsdottir, V., Strawbridge, R.J., Khan, H., Grallert, H., Mahajan, A., et al.; Wellcome Trust Case Control Consortium; Meta-Analyses of Glucose and Insulin-related traits Consortium (MAGIC) Investigators; Genetic Investigation of ANthropometric Traits (GIANT) Consortium; Asian Genetic Epidemiology Network–Type 2 Diabetes (AGEN-T2D) Consortium; South Asian Type 2 Diabetes (SAT2D) Consortium; DIAbetes Genetics Replication And Meta-analysis (DIAGRAM) Consortium (2012). Large-scale association analysis provides insights into the genetic architecture and pathophysiology of type 2 diabetes. Nat. Genet. *44*, 981–990.

Oshiro, N., Takahashi, R., Yoshino, K., Tanimura, K., Nakashima, A., Eguchi, S., Miyamoto, T., Hara, K., Takehana, K., Avruch, J., et al. (2007). The proline-rich Akt substrate of 40 kDa (PRAS40) is a physiological substrate of mammalian target of rapamycin complex 1. J Biol Chem. *282*, 20329–20339.

Nickelson, K.J., Stromsdorfer, K.L., Pickering, R.T., Liu, T.W., Ortinau, L.C., Keating, A.F., and Perfield, J.W., 2nd. (2012). A comparison of inflammatory and oxidative stress markers in adipose tissue from weight-matched obese male and female mice. Exp. Diabetes Res. *2012*, 859395.

Pettersson, U.S., Waldén, T.B., Carlsson, P.O., Jansson, L., and Phillipson, M. (2012). Female mice are protected against high-fat diet induced metabolic syndrome and increase the regulatory T cell population in adipose tissue. PLoS ONE *7*, e46057.

Polak, P., Cybulski, N., Feige, J.N., Auwerx, J., Rüegg, M.A., and Hall, M.N. (2008). Adipose-specific knockout of raptor results in lean mice with enhanced mitochondrial respiration. Cell Metab. *8*, 399–410.

Rolli-Derkinderen, M., Machavoine, F., Baraban, J.M., Grolleau, A., Beretta, L., and Dy, M. (2003). ERK and p38 inhibit the expression of 4E-BP1 repressor of translation through induction of Egr-1. J. Biol. Chem. *278*, 18859–18867.

Samuel, V.T., and Shulman, G.I. (2012). Mechanisms for insulin resistance: common threads and missing links. Cell *148*, 852–871.

Selman, C., Tullet, J.M., Wieser, D., Irvine, E., Lingard, S.J., Choudhury, A.I., Claret, M., Al-Qassab, H., Carmignac, D., Ramadani, F., et al. (2009). Ribosomal protein S6 kinase 1 signaling regulates mammalian life span. Science *326*, 140–144.

Sonenberg, N., and Hinnebusch, A.G. (2009). Regulation of translation initiation in eukaryotes: mechanisms and biological targets. Cell *136*, 731–745.

Stubbins, R.E., Najjar, K., Holcomb, V.B., Hong, J., and Núñez, N.P. (2012). Oestrogen alters adipocyte biology and protects female mice from adipocyte inflammation and insulin resistance. Diabetes Obes. Metab. *14*, 58–66.

Tominaga, R., Yamaguchi, S., Satake, C., Usui, M., Tanji, Y., Kondo, K., Katagiri, H., Oka, Y., and Ishihara, H. (2010). The JNK pathway modulates expression and phosphorylation of 4E-BP1 in MIN6 pancreatic beta-cells under oxidative stress conditions. Cell Biochem. Funct. *28*, 387–393.

Tsai, S., Sitzmann, J.M., Dastidar, S.G., Rodriguez, A.A., Vu, S.L., McDonald, C.E., Academia, E.C., O'Leary, M.N., Ashe, T.D., La Spada, A.R., and Kennedy, B.K. (2015). Muscle-specific 4E-BP1 signaling activation improves metabolic parameters during aging and obesity. J. Clin. Invest. *125*, 2952–2964.

Tseng, Y.H., Cypess, A.M., and Kahn, C.R. (2010). Cellular bioenergetics as a target for obesity therapy. Nat. Rev. Drug Discov. *9*, 465–482.

Tsukiyama-Kohara, K., Poulin, F., Kohara, M., DeMaria, C.T., Cheng, A., Wu, Z., Gingras, A.C., Katsume, A., Elchebly, M., Spiegelman, B.M., et al. (2001). Adipose tissue reduction in mice lacking the translational inhibitor 4E-BP1. Nat. Med. *7*, 1128–1132.

Um, S.H., Frigerio, F., Watanabe, M., Picard, F., Joaquin, M., Sticker, M., Fumagalli, S., Allegrini, P.R., Kozma, S.C., Auwerx, J., and Thomas, G. (2004). Absence of S6K1 protects against age- and diet-induced obesity while enhancing insulin sensitivity. Nature *431*, 200–205.

Um, S.H., D'Alessio, D., and Thomas, G. (2006). Nutrient overload, insulin resistance, and ribosomal protein S6 kinase 1, S6K1. Cell Metab. *3*, 393–402.

Walsh, D., Arias, C., Perez, C., Halladin, D., Escandon, M., Ueda, T., Watanabe-Fukunaga, R., Fukunaga, R., and Mohr, I. (2008). Eukaryotic translation initiation factor 4F architectural alterations accompany translation initiation factor redistribution in poxvirus-infected cells. Mol. Cell. Biol. *28*, 2648–2658.

Wang, L., Harris, T.E., and Lawrence, J.C., Jr. (2008). Regulation of proline-rich Akt substrate of 40 kDa (PRAS40) function by mammalian target of rapamycin complex 1 (mTORC1)-mediated phosphorylation. J Biol Chem. *283*, 15619–15627.

Weichhart, T., Costantino, G., Poglitsch, M., Rosner, M., Zeyda, M., Stuhlmeier, K.M., Kolbe, T., Stulnig, T.M., Hörl, W.H., Hengstschläger, M., et al. (2008). The TSC-mTOR signaling pathway regulates the innate inflammatory response. Immunity *29*, 565–577.

Williams, A.L., Jacobs, S.B., Moreno-Macías, H., Huerta-Chagoya, A., Churchhouse, C., Márquez-Luna, C., García-Ortíz, H., Gómez-Vázquez, M.J., Burtt, N.P., Aguilar-Salinas, C.A., et al.; SIGMA Type 2 Diabetes Consortium (2014). Sequence variants in SLC16A11 are a common risk factor for type 2 diabetes in Mexico. Nature *506*, 97–101.

Wu, J., Cohen, P., and Spiegelman, B.M. (2013). Adaptive thermogenesis in adipocytes: is beige the new brown? Genes Dev. *27*, 234–250.

Yang, Y., Wang, J., Qin, L., Shou, Z., Zhao, J., Wang, H., Chen, Y., and Chen, J. (2007). Rapamycin prevents early steps of the development of diabetic nephropathy in rats. Am. J. Nephrol. *27*, 495–502.

Zeyda, M., and Stulnig, T.M. (2007). Adipose tissue macrophages. Immunol. Lett. *112*, 61–67.